CHAPTER VII

IMPROVED *n*–PENTANE CONVERSION AND *p*–XYLENE SELECTIVITY USING Zn(II)IONS/SILICALITE–1 COATED ON Zn/HZSM–5 CATALYSTS

7.1 Abstract

ZnHZSM–5 based catalyst was studied in the transformation of *n*–pentane to the high selective *p*–xylene. In order to increase the *p*–xylene selectivity, the isomerization of *p*–xylene was suppressed by coating silicalite–1 layer on the external surface of ZnHZSM–5. Even the selectivity of *p*–xylene in xylenes was improved from 23 % to 57 %, the aromatics yield was found to be trade with *p*–xylene selectivity. With the propose to increase the catalytic activity while preserving the high *p*–xylene selectivity, the single site Zn(II) ions, playing a role as strong Lewis acid site was grafted on silicalite–1 layer. Due to its dehydrogenation activity, *n*–pentane feedstock was firstly converted to olefins on Zn(II)ions/Sil–1 then further aromatized in Zn/HZSM–5 catalyst. Thus the aromatics yield was significantly improved. Nonetheless, the single site Zn(II)ions also induced the generation of weak Brønsted acid sites on silicalite–1 layer, resulting in decreasing the *p*–xylene selectivity in xylenes to 43%. The roles of each Zn species and acidity in the conversion of *n*–pentane to *p*–xylene was studied by XPS and NH_3, IPA–TPD.

7.2 Introduction

Since *p*–xylene is one of the most valuable product in petrochemical industry, used as a raw materials of terephthalate and polyester, the catalysts development for the selective formation of *p*–xylene has been studied for decades. The acidic zeolite such as ZSM–5 [1-4], mordenite [5], zeolite Beta[6], Zeolite X [7], Zeolite Y [8], and MCM–22 [9], were widely studied as zeolite bases for the production of high *p*–xylene formation in the disproportionation and the alkylation of toluene with methanol. Compared with the others, ZSM–5 is very interesting because its pore size is favor the diffusion of *p*–xylene through out the channel than *o*– and *m*–xylene [9, 10]. However, due to the presence of its external Brønsted acid

site, the *p*–xylene, difussing out of the HZSM–5 channel was further isomerized to *o*– and *m*–xylene, leading to only 23% of *p*–xylene was detected.

Until now, many researchers have published the succesful methods to modify HZSM–5 catalyst for highly selective *p*–xylene such as the impregnation of MgO, phosphorous, or boron [3, 4]; deposition of inert silica on external Brønsted acid site by chemical vapor deposistion (CVD) [11], chemical liquid depostion (CLD) [2], and growthing silicalite–1 layer [12]. As expected, even the *p*–xylene selectivity was increased, the deposition of inert silica layer also decreased the catalytic activity. Thus to achieve both *p*–xylene selective and catalytic activity, the idea to create an active layer that only suppress the isomerization of xylene but still provided an active site to enhance the aromatization is studied in this work. Focusing in reaction pathway for aromatization of light hydrocarbon, The cracking of light paraffins feedstock over Brønsted acid site of HZSM–5 generated light olefins and paraffins. While light olefins acted as intermediates for producing aromatics, light paraffins were considered as inert unwanted by–products [13, 14]. It was expected that by introducing of dehydrogenation metal, the paraffins will firstly converted to olefins, further cracked to only olefins, intermediates in aromatic formation. The dehydrogenation metal such as Mo [15], La [16], Ga [17], Zn [18], Ni [19], Pt [20], and Ag [21] were loaded on HZSM–5 catalysts. Compared with the others, Zn loaded on HZSM–5 catalysts significantly improved aromatics yield [22]. It was proved that the Brønsted acid site of HZSM–5 catalyst was exchanged with the bivalent Zn cations, resulting in Zn at exchange site, performed as a strong Lewis acid site. This Zn species was widely accepted as an active species in the dehydrogenation of paraffins [22]. It is important to note again that the active site for isomerization of *p*–xylene is the external Brønsted acid site so the *p*–xylene selectivity should be preserved in the presence of only external Lewis acid site.

Herein, we dedicated an attempt to design the catalyst for highly selective *p*–xylene formation by using *n*–pentane as a feedstock. Zn/HZSM–5 catalyst (as a core) was coated with silicalite–1 layer (as a shell) to eliminate the external acid site. The shell was grafted with a single–site Zn^{2+}, using the strong electrostatic adsorption methodology. The external surface of HZSM–5 was expected to provide the Lewis acid site Zn^{2+} species, enhancing the dehydrogenation activity

of *n*–pentane. As a result, pentene will be passed through the Zn/HZSM–5 core. Focusing in the Zn/HZSM–5 core, starting with olefins will be must easier to convert to aromatics as compared with paraffins thus the aromatics yield should be increased.

7.3 Experiment

7.3.1 Catalyst Preparation

The NH_4ZSM–5 zeolite with SiO_2/Al_2O_3 ratio of 25 was calcined in air at 550 °C for 5 h the resulted catalyst was denoted as HZSM–5. The Zn^{2+} were loaded on the HZSM–5 catalyst by aqueous phase ion–exchange. Briefly, the HZSM–5 (4 g) was stirred in 0.05 M $Zn(NO_3)_2$ solution (100 mL) at 70 °C for 12 h. The ion–exchanged sample was washed with excess deionized water, dried overnight at 120 °C, after that calcined at 550 °C in air for 5 h, denoted as ZnHZSM–5 catalyst.

In order to coat silicalite–1 on the catalyst, Zn/HZSM–5 was used as a core. The precursor solution contained with TEOS, tetraprophylammonium hydroxide (TPAOH), ethanol (EtOH) and deionized water with the molar ratios of 0.5TPAOH: 120H_2O: 8EtOH: 2SiO_2. Approximately 1.0 g of Zn/HZSM–5 catalyst was immersed in 15 g of precursor solution. The solution was carried out in stainless steel vessel at 453 °C for 24 h without agitation. The products were rinsed with deionized water and dried over night at 363 K, then, calcined in air at 773 K for 6 h at a heating rate of 1 K/min. The resulted catalysts was denoted as Sil–1/ZnHZSM–5 catalyst.

The dehydrogenation layer was grafted on Sil–1/ZnHZSM–5 catalyst by using strong electrostatic adsorption methodology. Approximately 1.0 g of Sil–1/ZnHZSM–5 was suspended in 5 mL of deionized water. The solution was adjusted to pH 11 by using 30% ammonium hydroxide (NH_4OH). In a separate flask, 0.16 g of $Zn(NO_3)_2.6H_2O$ (Sigma Aldrich) was dissolved in 1.6 mL of deionized water. The pH of the solution also adjusted to be 11 using ammonium hydroxide. The solution was added to the catalyst solution and stir for 10 min. Then the mixed solution was allowed to settle for 5 min. The resultant slurry was rinsed several times with deionized water. The resulted catalyst was vacuum filtered, dried overnight at 125

°C, and calcined in air with a heating rate of 5 °C/min to 300 °C, maintained for 3 h. The catalyst was denoted as Zn(II)ions/Sil–1/ZnHZSM–5 catalyst.

7.3.2 Characterization

The specific surface area and micropore volume of the catalysts was measured by using Brumauer–Emmet–Teller (BET) method. The surface compositions and species of Zn on the surface was analyzed by X–ray photoelectron spectroscopy (XPS). The catalysts were conducted using a Kratos Ultra X–ray photoelctron spectrometer. The monochromatic AlKα was used as an X–ray source (anode HT = 15 kV). The XPS peaks were refernced to the binding energy of C (1s) peak at 285 eV. The temperature programmed desorption of isopropylamine (IPA–TPD) and ammonia (NH_3–TPD) were performed in a homemade flow apparatus using a quarter inch quartz tube reactor connected to an online MS detector (MKS Cirrus). The catalyst was heated under the He at 300 °C for 1 h after that cooled to 100 °C after which IPA (or NH_3) was introduced with the process gas until saturated. The temperature programmed desorption was carried out in the range of 100–700 °C at a ramp rate of 10 °C/min.

7.3.2 Catalytic Activity Testing

In each test, 0.1 g of catalyst was packed in a ¼" Pyrex fixed–bed reactor. The catalyst was heated under a flow of N_2 at 500 °C for 1 h. The *n*–pentane feed–stock was continuously injected from a syringe pump with WHSV of 10 h^{-1}. The condition reaction was at 500 °C under 1 atm of 20 mL/min of N_2 flow. The products were analyzed by gas chromatography using a Shimadzu 17A–GC equipped with an HP–PLOT/Al_2O_3 "*S*" deactivated capillary column. Conversion and product selectivity are calculated based on the following equations.

$$\text{Conversion (\%)} = \frac{\text{wt. of feed converted}}{\text{wt. of feed input}} \times 100$$

$$\text{Selectivity to product } i \text{ (\%)} = \frac{\text{wt. of product } i}{\text{Total wt. of products}} \times 100$$

7.4 Results and Discussion

7.4.1 Textural Properties

In order to confirm the existing of MFI structure, the crystallinity of the catalysts were investigated by XRD (Fig. 7.1). The results showed the comparable intensity of the peaks between HZSM–5 and ZnHZSM–5 catalysts, implying that the structure of HZSM–5 still be preserved after loading Zn. Focusing in coating ZnHZSM–5 with silicalite–1, the higher intensity of Sil–1/ZnHZSM–5 was detected. That might be due to the growth of silicalite–1 on ZnHZSM–5 catalyst, leading to the larger crystal size. It should be noted that instead of forming

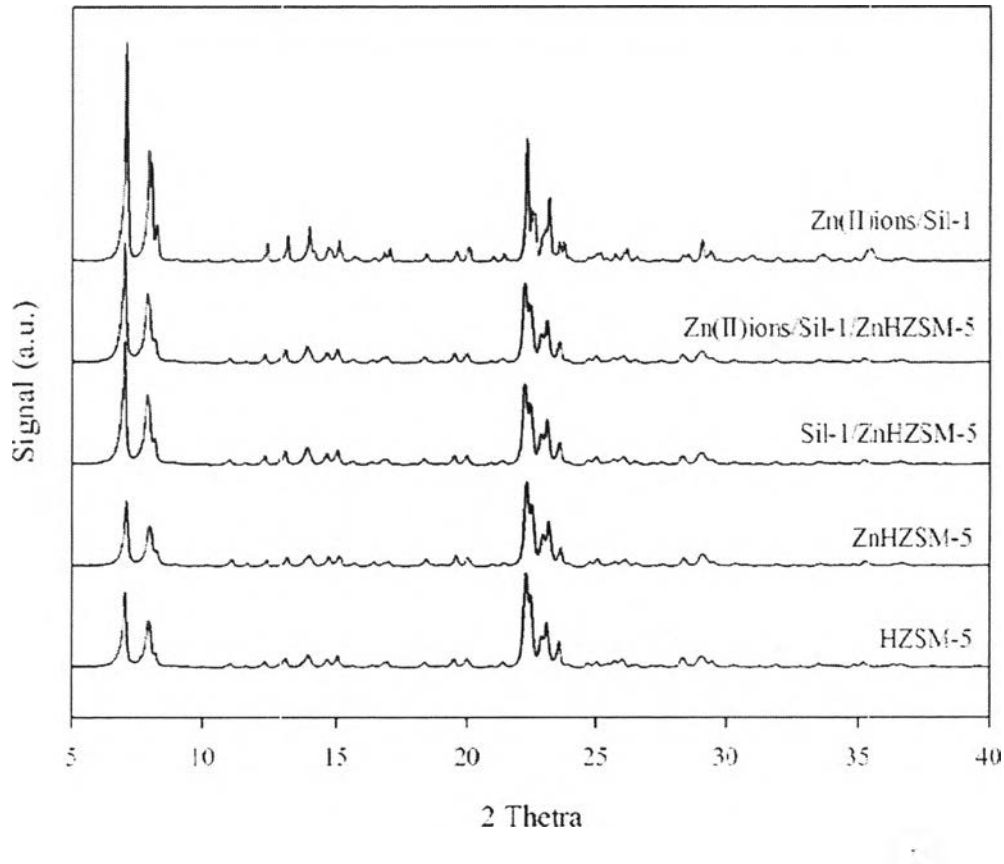

Figure 7.1 XRD patterns of HZSM–5, ZnHZSM–5, Sil–1/ZnHZSM–5, Zn(II)ions/Sil–1/ZnHZSM–5, and Zn(II)ions/Sil–1 catalysts.

silicalite–1 layer, the amorphous silica also could be formed with the characteristic peak at 2 thetra equal to 20°–30° region. However, XRD patterns showed only those assignable to MFI structure (2thetra = 7.9°, 8.8°, 23.1°, 23.9°, 24.4°), confirming the successful synthesis silicalite–1 coating on ZnHZSM–5 catalyst [23]. The total surface area and micropore volume was analyzed by BET method. The insignificant changing of total surface area and micropore volume was detected after the modification. Thus, it was reasonable to assume that the coating silicalite–1 did not block the Zn/HZSM–5 pores and Zn was highly dispersed on the catalyst.

Table 7.1 Total surface area and micropore volume of HZSM–5, ZnHZSM–5, Sil–1/ZnHZSM–5, and Zn(II)ions/Sil–1/ZnHZSM–5 catalysts

Catalysts	S_{BET} (m^2/g_{cat})	Vmicro (cm^3/g_{cat})
HZSM–5	358.3	0.229
ZnHZSM–5	344.2	0.223
Sil–1/ZnHZSM–5	357.5	0.207
Zn(II)ions/Sil–1/ZnHZSM–5	348.3	0.204

7.4.2 Analysis of Surface Compostion and Zn Species

The X–ray photoelectron spectroscopy (XPS) was used to investigate the surface composition and Zn species of the catalysts as exhibited in Table 7.2 and Fig. 7.2, respectively. Considering the surface composition of the catalysts (Table 7.2), Zn(II)ions/Sil–1 catalyst showed the higher amount of Zn as compared with expected metal loading (5 %). This result demonstrated the highly disperse of Zn on the surface of silicalite–1 support. As expected, in the case of ZnHZSM–5 catalyst, the low amount of Zn loading (0.6 %) was due to the limited exchangeability of HZSM–5 catalysts, agreed very well with our previous work [24, 25]. After coating silicalite–1 layer on ZnHZSM–5 catalyst, the surface composition confirmed the significant increase of Si content from 39.6% to 44.3% while the percentage of Al was decreased from 2.3% to 0.4%. By using strong electrostatic adsorption method,

XPS confirmed the successful of this method in grafting Zn(II)ions on silicalite–1 layer. Almost 12 % Zn was detected on the catalyst. It should be highlighted that the expected Zn loading should be only 3 % on the catalyst. The higher amount of Zn indicated that this Zn(II)ions was highly disperse on the external surface of silicalite–1 layer.

Table 7.2 Surface composition of Zn(II)ions/Sil–1, ZnHZSM–5, Sil–1/ZnHZSM–5, and Zn(II)ions/Sil–1/ZnHZSM–5 catalysts

Catalysts	% Metal loading (XPS)			
	Zn	O	Si	Al
Zn(II)ions/Sil–1	27.4	43.8	28.8	0
ZnHZSM–5	0.6	57.5	39.6	2.3
Sil–1/ZnHZSM–5	0.4	54.9	44.3	0.4
Zn(II)ions/Sil–1/ZnHZSM–5	11.9	50.1	37.9	0.1

The XPS deconvolutions of $Zn(2p_{3/2})$ on the catalysts are shown in Fig. 7.2. In order to confirmed the formation of different Zn species between the core ZnHZSM–5 and shell Zn(II)ions/Sil–1, Zn(II)ions/Sil–1, prepared by strong electrostatic adsorption method and ZnO were used as references. Agreed with our previous work [24, 25], ZnO showed the binding energy approximately 1021.5 eV (Fig. 7.2a). Considering the Zn(II)ions/Sil–1 catalyst prepared by strong electrostatic adsorption method. Under the basic solution, the hydroxyl groups of silicalite–1 are deprotonated, resulting in a negatively charged support. The depostion of Zn on the support was induced by the strong Coulombic attraction between the support and the Zn cation precursor. Thus the peak at 1022.2 eV of Zn(II)ions/Sil–1 dedicated to the formation of tetrahedrally cooordinated Zn(II) ions, chemisorbed into the three membered siloxane rigns of silicalite surface (Fig. 7.2b). This Zn species was previously confirmed by using UV–resonance Raman, XANES, and EXAFS spectra [26]. Focusing in the core ZnHZSM–5 catalyst, the XPS spectrum showed a higher

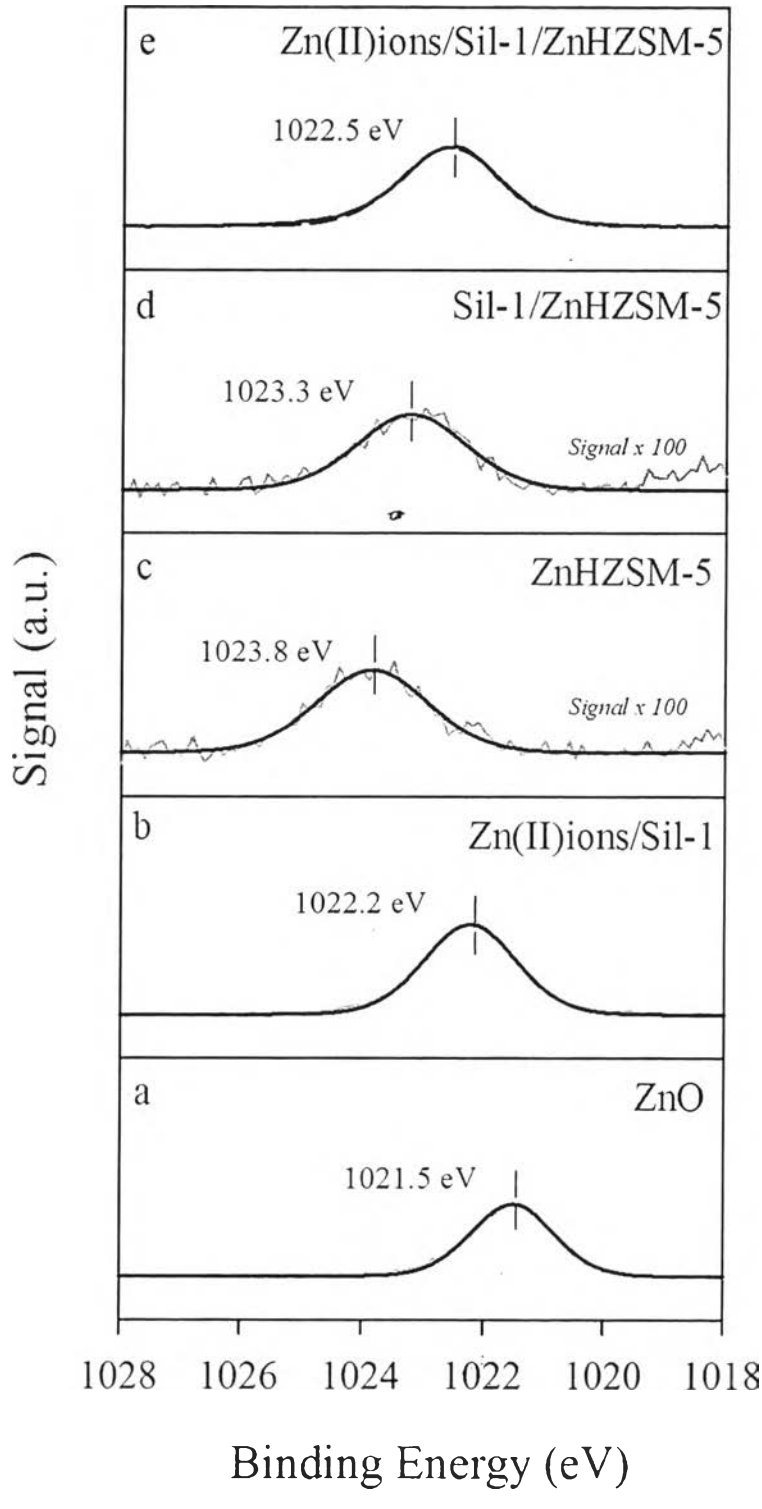

Figure 7.2 XPS (Zn ($2p_{3/2}$)) spectra of ZnO, Zn(II)ions/Sil–1, ZnHZSM–5, Sil–1/ZnHZSM–5, and Zn(II)ions/Sil–1/ZnHZSM–5 catalysts.

binding energy at 1023.8 eV (Fig. 7.2c), attributed to $(ZnOH)^+$ species. Compared with ZnO, the increase in binding energy was resulted from Zn^{2+} interacting with the electronegative oxygen framework. The introducing of silicalite–1 on ZnHZSM–5 catalyst was also effected to the electron affinity of the $(ZnOH)^+$ species. As shown in Fig. 7.2d, the shifting to the lower binding energy at 1023.3 eV might be due to the decrease of Brønsted acid site, led to the decrease of electron affinity of the catalyst.

The generation of Zn(II)ions on Zn(II)ions/Sil–1/ZnHZSM–5 catalyst was confirmed by XPS (Fig. 7.2e). The shifting to lower binding energy as compared with $(ZnOH)^+$ species (1023.8 eV) of ZnHZSM–5 catalyst, demonstrated that the further introducing Zn on Sil–1/ZnHZSM–5 catalyst resulted in the formation of different Zn species. The comparable binding energy of Zn on both Zn(II)ions/Sil–1/ZnHZSM–5 and Zn(II)ions/Sil–1 led to the conclusion that the Zn species deposited on the external surface of Zn(II)ions/Sil–1/ZnHZSM–5 catalyst was tetrahedzedrally cooordinated Zn(II) ions stabilized on three membered siloxane rigns of silicalite–1. One might concerned that the deposition of Zn on Zn(II)ions/Sil–1/ZnHZSM–5 might form ZnO species. However as proved by XPS, the obviously different of Zn ($2p_{3/2}$) spectra between Zn(II)ions/Sil–1/ZnHZSM–5 and ZnO confirmed the disappearance of ZnO species.

7.4.3 The Acidic Properties

Total acidity and acid strength of the catalysts was studied by using temperature programmed desorption of ammonia (NH_3–TPD) as shown in Fig 7.3. The NH_3–TPD profile of the catalyst shows three type of desorption peaks, differentiated by using temperature as listed in Table 7.3. The quantities of strong, medium, and weak acid site are measured by the amount of ammonia desorbed at 300–550, 200–300, and 120–200 °C, respectively. Compared with HZSM–5, the expense of weak and strong acid sites was found with the increase of the medium acid site after loading Zn on HZSM–5 catalyst. As previously reported, the Zn^{2+} cations exchanged with the strong acid site and stabilized at the $(AlO)^-$ of the zeolite, exhibiting as a medium acid sites [27]. The significant decrease of total acidity was detected after the deposition of silicalite–1 on ZnHZSM-5 catalyst. It should be noted

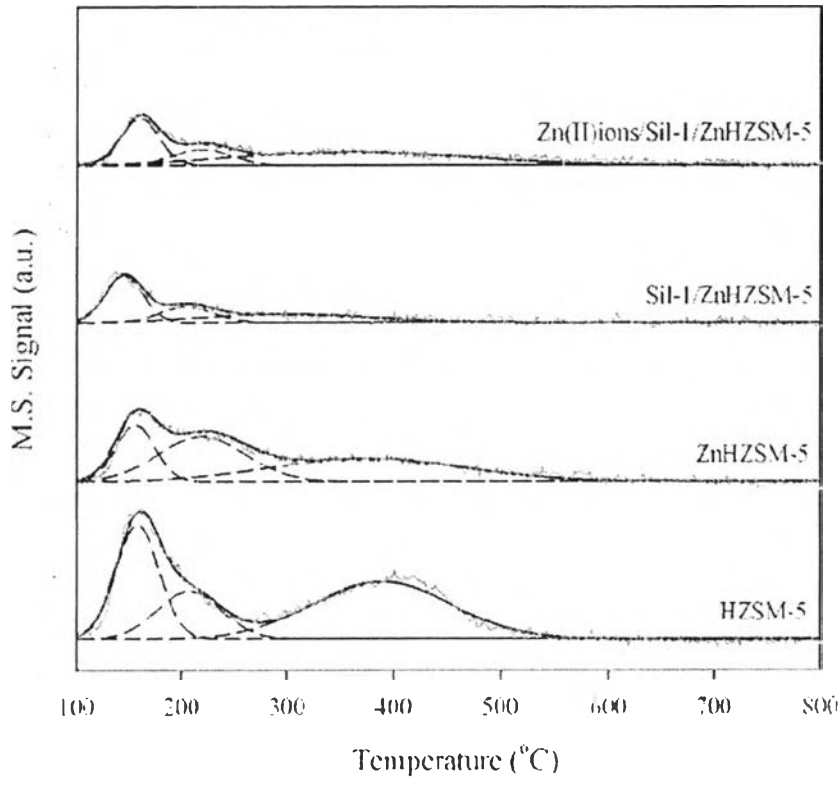

Figure 7.3 Ammonia–TPD (NH_3–TPD) profiles of HZSM–5, ZnHZSM–5, Sil–1/ZnHZSM–5, and Zn(II)ions/Sil–1/ZnHZSM–5 catalysts. The mass monitored was ammonia (*m/e*=17).

Table 7.3 The total acidity, detected by NH_3–TPD of HZSM–5, ZnHZSM–5, Sil–1/ZnHZSM–5, and Zn(II)ions/Sil–1/ZnHZSM–5 catalysts

Catalysts	Total acidity (μmol/g)			
	Weak	Medium	Strong	Total
HZSM–5	318	199	499	1015
ZnHZSM–5	143	250	283	676
Sil–1/ZnHZSM–5	113	53	91	257
Zn(II)ions/Sil–1/ZnHZSM–5	114	57	201	372

that due to the absence of Al in MFI structure of silicalite-1, the strong acidity should not exist thus resulting in lower total acidity of Sil–1/ZnHZSM–5 catalyst. However, after introducing the Zn(II) ions into the Sil–1/ZnHZSM–5 catalyst, the significant increase of strong acid site from 91 to 201 μmol/g was detected. The result was plausible to assume that Zn(II)ions exhibited as a strong acid site. Agreed very well with previous work studied by Schweitzer and co–workers [26], reported the formation of strong Lewis acid properties of Zn(II)ions over SiO_2 catalyst.

The Brønsted acid properties of the catalysts were studied by using temperature programmed desorption of isopropylamine (IPA–TPD). As shown in Fig. 7.4, the propylene (*m/e=41*) desorption at temperature approximately 350 °C was dedicated to the strong Brønsted acid sites of HZSM–5. After loading Zn, the exchange of Zn cations with the strong Brønsted acid sites resulted in lower the strong Brønsted acidity from 535 to 232 μmol/g (Table 7.4). This result accepted well with the XPS and NH_3–TPD that indicated the formation of $(ZnOH)^+$ species at exchangeable site. As expected, loading silicalite–1 on ZnHZSM–5 catalyst exhibited a significance influence on the Brønsted acidity. The decrease in Brønsted acidity was in line with the quantitative analysis of XPS (Table 7.2) that confirmed the decrease of Al content on the surface, implying to the success in deposition of silicalite–1 on ZnHZSM–5 catalyst. In addition, focusing in the strong Brønsted acid site at 350 °C, the significant lower in its acidity might also came from the narrowing of ZnHZSM–5 pore, hindering the adsorption of IPA. In contrast with Sil–1/ZnHZSM–5 catalyst, introducing Zn(II)ions on the Sil–1/ZnHZSM–5 catalyst, the weak Brønsted acid site (360–520 °C) significantly increased, resulting in increase the total Brønsted acidity from 134 to 284 μmol/g. The generation of this new weak Brønsted acid site might be resulted from the silanol group on silicalite–1 that is induced by the present of strong Lewis acid Zn(II)ions species. As reported by E.J.M. Hensen and co–workers, the interaction of silanol group with strong Lewis acid arised the weaker Brønsted acid site [28]. It is important to highlight that the increase in Brønsted acidity only found at high temperature peaks. The insignificant changing of the strong Brønsted acidity (350 °C) indicated that the Zn cations, loaded in this step only stabilized as Zn(II)ions on silicalite–1 layer, without exchanging with the proton of HZSM–5 zeolite.

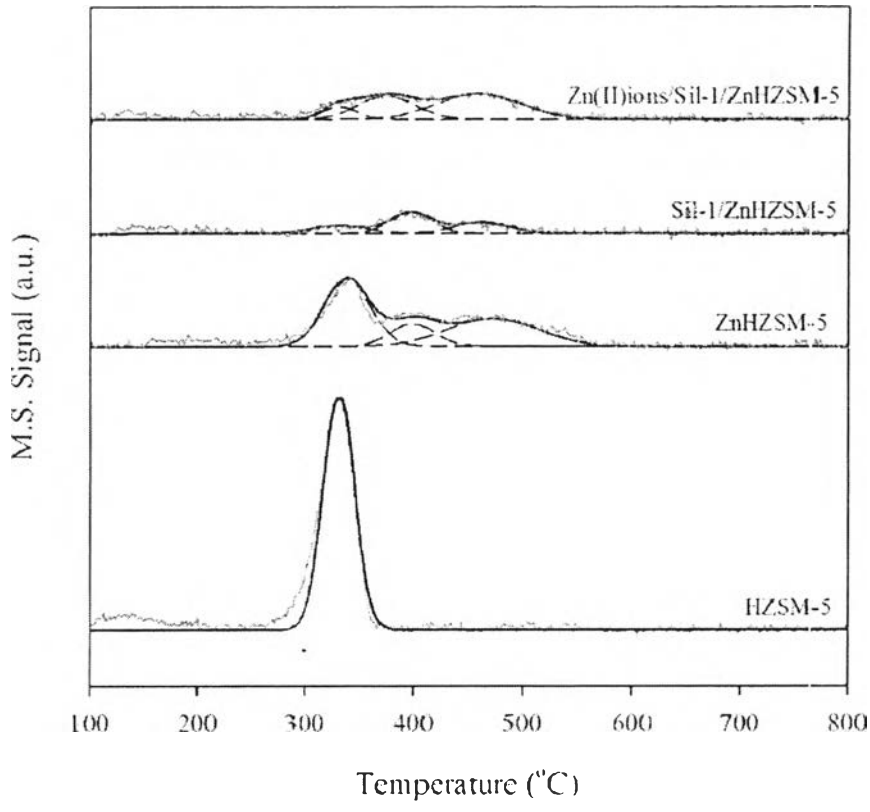

Figure 7.4 Isopropylamine–TPD (IPA–TPD) profiles of HZSM–5, ZnHZSM–5, Sil–1/ZnHZSM–5, and Zn(II)ions/Sil–1/ZnHZSM–5 catalysts. The mass monitored was ammonia (*m/e*=41).

Table 7.4 The total Brønsted acidity, detected by IPA–TPD of HZSM–5, ZnHZSM–5, Sil–1/ZnHZSM–5, and Zn(II)ions/Sil–1/ZnHZSM–5 catalysts

Catalysts	Brønsted acidity (μmol/g)			
	330–360 °C	360–420 °C	420–520 °C	Total
HZSM–5	535	0	0	535
ZnHZSM–5	232	74	188	494
Sil–1/ZnHZSM–5	32	58	44	134
Zn(II)ions/Sil–1/ZnHZSM–5	31	96	156	284

7.4.3 The Catalytic Activity

The catalytic activity was studied in the aromatization of *n*–pentane. As shown in Table 7.5, unmodified HZSM–5 catalyst exhibited 57.5 % of *n*–pentane conversion. The paraffins selectivity was found as a main composition at 50.4 % while the BTX aromatics was formed only 9.9 %. However, the aromatics was significantly improved after introducing Zn on HZSM–5 catalyst. The result showed the increase in aromatics selectivity to 24.5 % with the expense of the paraffins. As widely accepted [24, 25, 27], the $(ZnOH)^+$, stabilized at exchangeable site promoted the dehydrogenation of paraffins to olefins while the oligomerization and aromatization of resulting olefins were achieved on the Brønsted acid site of HZSM–5. To improve the *p*–xylene selectivity, silicalite–1 was coated on ZnHZSM–5 catalyst denoted as Sil–1/ZnHZSM–5. Not unexpectedly, the selectivity of *p*–xylene in mixed xylenes was improved, from 23 % over ZnHZSM–5 to 57 %. However as confirmed by IPA–TPD (Table 7.4), the dramatically decrease of Brønsted acidity resulted in the lower *n*–pentane conversion and also aromatics selectivity to 17.3 % and 18.6 % respectively.

With the propose to increase the aromatics yield, Zn(II)ions, expected to behave as a dehydrogenation layer was later grafted on Sil–1/ZnHZSM–5 catalyst. In order to understand the catalytic activity of Zn(II)ions, the same reaction condition in the conversion of *n*–pentane was tested on Zn(II)ions/Sil–1 catalysts, as shown in Table 5. Due to the lack of strong Brønsted acid site, the lower *n*–pentane conversion was noticed at 13.6 %. However, the remarkably high olefins selectivity (69.6 %) indicated that even in the environment that lack of $(AlO)^-$, Zn^{2+} stabilized on three membered siloxane rigns of silicalite–1 also performed an extraordinary high performance in dehydrogenation of paraffins. Considering in product distribution, the high amount of pentenes selectivity (12.3 %) implied that *n*–pentane was firstly dehydrogenated to pentene, further cracked to ethylene and propylene. As the high amount of light olefins were detected, we believed that the weak Brønsted acid, induced by Zn(II)ions as previously confirmed by IPA–TPD was an active site for this cracking reaction. In line with this explanation, small amount of aromatics (11.8 %) was also generated over this weak Brønsted acid site.

Table 7.5 Product distribution of *n*–pentane transformation over HZSM–5, ZnHZSM–5, Sil–1/ZnHZSM–5, Zn(II)ions/Sil–1, and Zn(II)ions/Sil–1/ZnHZSM–5 catalysts

Product distribution (wt %)	Catalysts				
	HZSM–5	ZnHZSM–5	Sil–1/ZnHZSM–5	Zn(II)ions/Sil–1	Zn(II)ions/ Sil–1/ZnHZSM–5
Conversion	**57.5**	**47.5**	**17.3**	**13.6**	**33.1**
Product selectivity					
Paraffins	**50.4**	**44.9**	**26.4**	**18.6**	**22.6**
Methane	2.3	3.2	2.3	2.3	2.8
Ethane	9.9	8.0	7.8	6.8	8.3
Propane	28.8	20.7	10.8	5.5	8.0
Butanes	9.4	13.0	5.5	4.0	3.5
Olefins	**39.7**	**30.6**	**54.9**	**69.6**	**51.0**
Ethylene	12.6	9.0	15.2	16.3	17.3
Propylene	15.9	11.4	20.3	26.8	21.5
Butenes	9.4	9.2	13.3	14.2	8.8
Pentene	1.8	1.0	6.1	12.3	3.4
BTX aromatics	**9.9**	**24.5**	**18.6**	**11.8**	**26.3**
Benzene	1.2	5.4	4.8	2.5	6.7
Toluene	4.3	11.7	7.5	5.1	10.3
Ethylbenzene	0.0	0.9	0.8	0.0	1.1
Xylenes	4.4	6.5	5.5	4.2	8.2
Selectivity of *p*–xylene in xylenes	**23**	**23**	**57**	**-**	**43**

Reaction conditions: Atmospheric pressure, 500 °C, WHSV = 10 h^{-1}, and TOS = 80 min.

The dehydrogenation layer Zn(II)ions was successfully coated on Sil–1/ZnHZSM–5 denoted as Zn(II)ions/Sil–1/ZnHZSM–5 catalyst and its catalytic activity is shown in Table 7.5. As compared with Sil–1/ZnHZSM–5 catalyst, the *n*–pentane conversion and aromatics selectivity notably increased to 33.1 % and 26.3 % respectively. From the result, it is plausible to explain that the addition of Zn(II)ions resulted in converting *n*–pentane to olefins. The resulted olefins passed through to the ZnHZSM–5 core, where the aromatization took place. Starting with olefins the aromatic formation must be gained easier. Even it is possible that the generation of weak Brønsted acid site on Zn(II)ions/Sil–1 layer might increase the *n*–pentane conversion, the isomerization of xylenes isomer was also enhanced led to the decrease of *p*–xylene selectivity to only 43 %.

7.5 Conclusion

The selective formation of *p*–xylene from the conversion of *n*–pentane was studied over modified catalysts. Compared with HZSM–5 catalyst, the presence of $(ZnOH)^+$ species in ZnHZSM–5 significantly increased aromatics yield. However to increase the *p*–xylene selectivity, the external Brønsted acid site of ZnHZSM–5 catalyst must be eliminated. Thus ZnHZSM–5 catalyst was used as a core, coated with silicalite–1 layer to suppress the isomerization of *p*–xylene. Even the *p*–xylene selectivity was increased, the decrease of Brønsted acidity also lowered the aromatics yield. With the aim to improve catalytic activity while preserving *p*–xylene selectivity, the Sil–1/ZnHZSM–5 catalyst was later grafted with Zn cations by using strong electrostatic adsorption method. The XPS confirmed the formation Zn(II)ions on silicalite–1 layer, clearly differentiated from $(ZnOH)^+$ species. The high performance in dehydrogenation was found over this Zn species, thus aromatics selectivity was significantly improved with high selectivity of *p*-xylene over Zn(II)ions/Sil–1/ZnHZSM–5 catalyst. The results indicated that Zn(II)ions on silicalite–1 play a role in converting *n*–pentane to olefins. Whereas, $(ZnOH)^+$ in ZnHZSM–5 catalyst performed the aromatization of resulted olefins.

7.6 Acknowledgements

The authors thank for the financially supported by the Center of Excellence on Petrochemical and Materials Technology and the Petroleum and Petrochemical College, Chulalongkorn University, Thailand.

7.7 References

1 G. Mirth, J. Cejka, J.A. Lercher, J. Catal. 139 (1993) 24.

2 J. Cejka, N. Zilkova, B. Wichterlova, G. Elder-Mirth, J.A. Lercher, Zeolites 17 (1996) 265.

3 N.Y. Chen, W.W. Kaeding, F.G. Dwyer, J. Am. Chem. Soc. 101 (1979) 6783.

4 W.W. Kaeding, C. Chu, L.B. Young, B. Weinstein, S.A. Butter, J. Catal. 67 (1981) 159.

5 R. Mantha, S. Bhatia, M.S. Rao, Ind. Eng. Chem. Res. 30 (1991).

6 A.E. Palomares, G. Elder-Mirth, J.A. Lercher, J. Catal. 168 (1997) 442.

7 T. Yashima, H. Ahmad, K. Yamazaki, M. Katsuta, N. Hara, J. Catal. 16 (1970) 273.

8 E. Dumitriu, V. Hulea, S. Kaliaguine, M.M. Huang, Appl. Catal. A 135 (1996) 57.

9 P. Wu, T. Komatsu, T. Yashima, Micropor. Mesopor. Mater. 22 (1998) 343.

10 P. Ratnasarmy, R.N. Bhat, S.K. Pokhriyal, J. Catal. 119 (1989) 65.

11 A.B. Halgeri, J. Das, Catal. Today 73 (2002) 65.

12 D.V. Vu, M. Miyamoto, N. Nishiyama, Y. Egashira, K. Ueyama, J. Catal. 243 (2006) 389.

13 D. Bhattacharya, S. Sivasanker, Appl. Catal. A 141 (1996) 105.

14 B.H. Davis, Catal. Today 53 (1999) 443.

15 F. Solymosi, J. Cserenyi, A. Szoke, T. Bansagi, A. Oszko, J. Catal. 165 (1997) 150.

16 Y.W. Zhang, Y.M. Zhou, H. Liu, Y. Wang, Y. Xu, P.C. Wu, Appl. Catal. A 333 (2007) 202.

17 G. Giannetto, R. Monque, R. Galiasso, Catal. Rev.: Sci. Eng. 36 (1994) 271.

18 J.A. Biscardi, G.D. Meitzner, E. Iglesia, J. Catal. 179 (1998) 192.

19 C.L. Yin, R.Y. Zhao, C.G. Liu, Fuel 84 (2005) 701.

20 O.V. Chetina, T.V. Vasina, V.V. Lunin, Appl. Catal. A 131 (1995) 7.

21 Y. Ono, Catal. Rev.: Sci. Eng. 34 (1992) 179.

22 L. Yu, S. Huang, S. Zhang, Z. Liu, W. Xin, S. Xie, L. Xu, ACS. Catal. 2 (2012) 1203.

23 Y. Wu, J. Li, Y. Chai, H. Guo, C. Liu, J. Membrane Sci. 496 (2015) 70.

24 S. Tamiyakul, W. Ubolcharoen, D.N. Tungasmita. S. Jongpatiwut, Catal. Today 256 (2015) 325.

25 S. Tamiyakul, S. Anutamjarikun, S. Jongpatiwut, Catal. Commun. 74 (2016) 49.

26 N.M. Schweitzer, B. Hu, U. Das, H. Kim, J. Greeley, L.A. Curtiss, P.C. Stair, J.T. Miller, A.S. Hock, ACS. Catal. 4 (2014) 1091.

27 X. Niu, J. Gao, Q. Miao, M. Dong, G. Wang, W. Fan, Z. Qin, J. Wang, Micropor. Mesopor. Mater. 197 (2014) 252.

28 E.J.M. Hensen, D.G. Poduval, V. Degirmenci, D.A.J.M. Ligthart, W. Chen, F. Mauge, M. Rigutto, J.A.R.V. Veen, J. Phys. Chem. C 116 (2012) 21416.